

Transient carbon monoxide poisoning of a polymer electrolyte fuel cell operating on diluted hydrogen feed

Krishan Kumar Bhatia, Chao-Yang Wang*

*Electrochemical Engine Center, Department of Mechanical and Nuclear Engineering,
The Pennsylvania State University, University Park, PA 16802, USA*

Received 11 November 2003; received in revised form 25 January 2004; accepted 26 January 2004

Abstract

The transient behavior of a 50 cm² PEM fuel cell fed on simulated reformat containing diluted hydrogen and trace quantities of carbon monoxide (CO) was experimentally investigated. It was found that the overall cell performance throughout the CO poisoning process can be described with a lumped model of hydrogen and CO adsorption, desorption, and electro-oxidation coupled with a current–voltage relationship for fuel cell performance. It was shown that while hydrogen dilution alone does not have an appreciable effect on cell polarization, in the presence of trace amounts of CO, hydrogen dilution amplifies the problem of CO poisoning. This is a result of the diluent reducing the partial pressure of reactants in the anode feed stream, thus retarding the already CO-impaired hydrogen adsorption onto the catalyst surface. In a diluted hydrogen stream, even low CO concentrations (i.e. 10 ppm), which are traditionally considered safe for PEM fuel cell operation, were found to be harmful to cell performance.

© 2003 Elsevier Ltd. All rights reserved.

Keywords: Fuel cell; Hydrogen; Carbon monoxide poisoning; Reformer; Automotive

1. Introduction

Increasing awareness regarding environmental issues and depleting energy reserves has prompted research into diverse possibilities for powering tomorrow's vehicles. More recently, a great deal of attention has been focused towards the use of hydrogen for on-board fuel cells. Currently, the most widely used method of hydrogen generation is via steam reforming of natural gas [1]. All hydrocarbon reforming methods, whether it be steam reforming, partial oxidation, or autothermal reforming, generate an effluent which is dilute in hydrogen and contains varying amounts of trace carbon monoxide (CO). Some form of hydrocarbon reforming, whether on-board or off-board the vehicle, will be the fuel source for these advanced vehicles until carbon-free pathways for hydrogen generation are developed. The effluent stream from reformers, which contains CO and is dilute in hydrogen, can be purified using a variety of methods (i.e. pressure swing adsorption, catalytic preferential oxidation,

etc.), but in order to produce large quantities of economical, fuel cell grade hydrogen, the exact performance and durability effects of dilution and trace carbon monoxide must be known.

Depending on the hydrocarbon feedstock, reformer effluent can contain hydrogen as dilute as 32% [2]. The effect of dilution with a CO-free feed gas has been studied, and is widely understood at a fundamental level [3]. The decrease in cell polarization at increased current draw is attributed to the reduction in average hydrogen concentration in the anode flow field, thus requiring a larger anode overpotential to maintain the hydrogen oxidation reaction at a specified current density. Fortunately, due to the anode normally exhibiting very fast kinetics, the inlet hydrogen concentration has to be very dilute to have an appreciable effect on cell polarization. Carbon monoxide, however, is a known fuel cell catalyst poison even in trace amounts, and is preferentially adsorbed on the catalyst surface. CO concentrations as low as 10 ppm are extremely detrimental to fuel cell performance.

Gottesfeld and Pafford [4] conducted some of the earliest work on CO poisoning of fuel cells. In that work, the poisoning phenomenon was documented with CO levels varying

* Corresponding author. Tel.: +1-814-863-4762;

fax: +1-814-863-4848.

E-mail address: cwx31@psu.edu (C.-Y. Wang).

from 10 to 100 ppm. A membrane remediation technique using oxygen injection into the anode feed stream was also presented [4]. Springer et al. [5] have developed a kinetic model for hydrogen and CO adsorption and subsequent electro-oxidation. This model was then solved under steady state conditions for the fractional surface coverage of hydrogen and CO, as well as the cell current. It was calculated that under conditions of CO-free feed gas, the performance loss should not exceed 10% of full stack power with hydrogen concentrations as low as 40% [5]. However, in the presence of CO levels as low as 10 ppm, the losses start to become significant, and were calculated to be exaggerated even further under the combined conditions of anode feed gas having a low hydrogen concentration and trace amounts of CO. This is in agreement with findings by Divisek et al. [6], who showed that with a 75% hydrogen, 25% CO₂, and 100 ppm CO fuel feed, the steady state cell performance was lower than that with a 100% hydrogen, 100 ppm CO feed. The model developed by Springer et al. has also been extended and modified several times by other researchers [7,8].

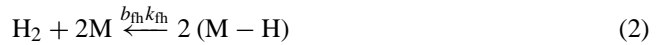
The transient process of poisoning in a hydrogen/oxygen fuel cell has also been experimentally studied [9]. Oetjen et al. [9] found that for Pt catalysts and feed gas containing 100 ppm CO, performance degradation was observable even after 5 min of exposure, with the cell reaching the fully steady state poisoned condition after roughly 2 h. However, the feed consisted of 100% hydrogen with trace CO. Moreover, oxygen was used on the anode instead of air. Murthy et al. [10] found that a small amount of air injection in the anode feed stream can significantly reduce the transient decay rate of fuel cell polarization during the poisoning process. Aside from cell polarization measurements, other methods, such as electrochemical impedance spectroscopy, have been used to study the CO poisoning process [11].

This past work shows that while much is known about steady state poisoning with a 100% hydrogen feed containing trace amounts of CO, there is a lack of experimental data to quantify the transient CO poisoning process with diluted hydrogen, which is the actual case for fuel cells being fed a hydrocarbon reformat gas. In addition, even less is known fundamentally about the transient process of fuel cell poisoning with reformat gas. Understanding this process is critical in determining the minimum purity requirements for anode fed gas as well as developing any sort of poisoning remediation method.

2. Theoretical analysis

Springer et al. present the following set of reactions to describe the adsorption, desorption, and electro-oxidation of hydrogen and CO on the catalyst surface, where M represents a free catalyst site. These assume that any inert species, such as nitrogen or carbon dioxide, which may be diluting the anode feed stream, do not participate in the surface ad-

sorption chemistry [5].



From this, a set of kinetic equations describing the rate of change of hydrogen and CO coverage on the catalyst surface in terms of the rates of adsorption, desorption, and electro-oxidation can be written. Springer et al. drop the rate of change of surface coverage with time in order to find the steady state cell polarization. However, here we are interested in the transient cell behavior, and thus include these terms in our calculations. These kinetics equations developed by Springer et al. have been modified to assume that the adsorption and desorption of species are first order in nature. Also, the charge transfer coefficient, α , is assumed to be equal to 0.5, which reduces the general Butler–Volmer equation for electro-oxidation into a hyperbolic sine relationship.

$$\rho \frac{d\theta_{\text{h}}}{dt} = k_{\text{fh}}x_{\text{h}}P(1 - \theta_{\text{h}} - \theta_{\text{c}}) - b_{\text{fh}}k_{\text{fh}}\theta_{\text{h}} - 2k_{\text{eh}}\theta_{\text{h}}\sinh\left(\frac{\eta_{\text{a}}}{RT/\alpha F}\right) \quad (7)$$

$$\rho \frac{d\theta_{\text{c}}}{dt} = k_{\text{fc}}x_{\text{c}}P(1 - \theta_{\text{h}} - \theta_{\text{c}}) - b_{\text{fc}}k_{\text{fc}}\theta_{\text{c}} - 2k_{\text{ec}}\theta_{\text{c}}\sinh\left(\frac{\eta_{\text{a}}}{RT/\alpha F}\right) \quad (8)$$

Eqs. (7) and (8) balance the rate of change of hydrogen and CO fractional surface coverage, θ_{h} and θ_{c} , with respect to time against the respective rates of adsorption, desorption, and electro-oxidation from the catalyst surface. The terms ρ , x_{h} , x_{c} , and η_{a} represent the molar area density of catalyst sites times Faraday's constant, hydrogen mole fraction, CO mole fraction, and anode overpotential respectively.

The hydrogen electro-oxidation term was then re-written in terms of hydrogen current, i . The CO electro-oxidation term was dropped due to its relatively small magnitude at the cell voltages considered here as compared to the CO adsorption and desorption terms. An additional equation for cell voltage in terms of current was also needed to close the system. This zero-dimensional, “black box” model for cell voltage assumes Tafel kinetics on the cathode and linear

Table 1
Constants used for solving kinetics model

b_{fc}	2.75×10^{-7} atm
b_{fh}	0.5 atm
F	96485 C mol ⁻¹
i_{oc}	7.0×10^{-4} A cm ⁻²
k_{eh}	4 A cm ⁻²
k_{fc}	10 A cm ⁻² atm ⁻¹
k_{fh}	100 A cm ⁻² atm ⁻¹
P	3 atm absolute
R	8.314 J mol ⁻¹ K ⁻¹
R_{ohmic}	0.3 Ω cm ²
T	353 K
V_{cell}	0.6 V
V_o	1.2 V
α	0.5
ρ	0.1 C cm ⁻²

ohmic losses through the cell. This results in the following set of equations:

$$\rho \frac{d\theta_h}{dt} = k_{fh}x_h P(1 - \theta_h - \theta_c) - b_{fh}k_{fh}\theta_h - i \quad (9)$$

$$\rho \frac{d\theta_c}{dt} = k_{fc}x_c P(1 - \theta_h - \theta_c) - b_{fc}k_{fc}\theta_c \quad (10)$$

$$V_{cell} = V_o - \eta_a - \eta_c - \eta_{ohmic} \quad (11)$$

Where the terms in Eq. (11) are given by:

$$\eta_a = \frac{RT}{\alpha F} \sinh^{-1} \left(\frac{i}{2k_{eh}\theta_h} \right) \quad (12)$$

$$\eta_c = \frac{RT}{\alpha F} \ln \left(\frac{i}{i_{oc}} \right) \quad (13)$$

$$\eta_{ohmic} = iR_{ohmic} \quad (14)$$

Eqs. (9)–(14) can be solved numerically for the time variation of fractional surface coverage of hydrogen, CO, and the cell current at a constant cell voltage. This theoretical model will be used later to compare and explain the experimental results. Values for the constants in Eqs. (9)–(14) are given in Table 1. Values for pressure, temperature, and cell voltage represent the actual operating conditions that the experiments were conducted under. Values for the ohmic resistance, R_{ohmic} , and cathode exchange current density, i_{oc} , were found from curve fits to baseline cell performance data. Values for all of the kinetic parameters were taken from those used previously in the literature [5], except for b_{fc} and k_{fh} . Springer et al. noted that these two kinetic parameters are functions of the fractional CO coverage, however, for the purposes of this study, they are assumed to be constant. The values for these two parameters were chosen to best match the transient cell performance data. These numeric values for these two parameters fall within the range of variability that has been previously reported [5].

3. Experimental

The experimental tests were performed in a 50 cm² titanium fuel cell supplied by Lynntech Industries Ltd. (College Station, TX). Both anode and cathode flow fields consisted of 6 parallel channels following a serpentine path to cover the 50 cm² of active area. The membrane electrode assemblies (MEAs), also supplied by Lynntech Industries, were composed of 40% platinum on carbon, Nafion[®] 112, with a platinum catalyst loading of 0.5 mg cm⁻² on each side. Although a platinum-ruthenium combination is known to be more CO-tolerant, pure platinum was chosen as the anode catalyst in order to undertake a basic study of the CO poisoning mechanism. The MEA also had an ELAT gas diffusion layer pressed on top of the catalyst surface.

The polarization measurements were taken using an Arbin Instruments (College Station, TX) fuel cell test station and electronic load bank. Both anode and cathode feed streams were fully saturated with water at 80 °C and maintained at that temperature while being fed to the cell. All numbers for the hydrogen dilution in the anode feed streams are based on the dry gas condition before saturation with water at 80 °C. The flow rates of both streams were continually modified with respect to the instantaneous current draw to maintain a molar flow level corresponding to a constant stoichiometry condition of 1.5 and 2.5 on the anode and cathode respectively. The cell itself was kept at 80 °C and pressurized to 300 kPa (absolute) on both anode and cathode sides. Tests were performed under a variety of hydrogen dilution levels and CO concentrations. During these tests, the cell polarization was measured at specific times throughout the CO poisoning process. Between polarization scans, the cell was maintained at a current draw corresponding to a constant cell potential of 600 mV.

4. Results and discussion

The 50 cm² fuel cell was tested under a variety of conditions to simulate a wide range of actual reformate gases. First, the cell was tested with CO-free feed gas consisting of 100% hydrogen and then 40% hydrogen, balanced with nitrogen (Fig. 1). Both CO-free cases do not exhibit any transient performance loss, and thus only the steady state cell polarization is shown. As shown, almost no performance loss is observable even with the low hydrogen concentration feed gas. Then, the cases of anode feed gas having varying levels of CO and hydrogen dilution were considered. Figs. 2 and 3 show the entire cell polarization at various times throughout the poisoning process for an anode feed of 100 and 40% hydrogen, respectively, with 10 ppm CO. The curves at 120 min represent the fully poisoned, steady state cell polarization. Similar curves for 100 and 40% hydrogen with 100 ppm CO are shown in Figs. 4 and 5 respectively. Fig. 6 shows the current obtainable at a cell voltage of 0.6 V versus time for all four feed gas cases considered here, as

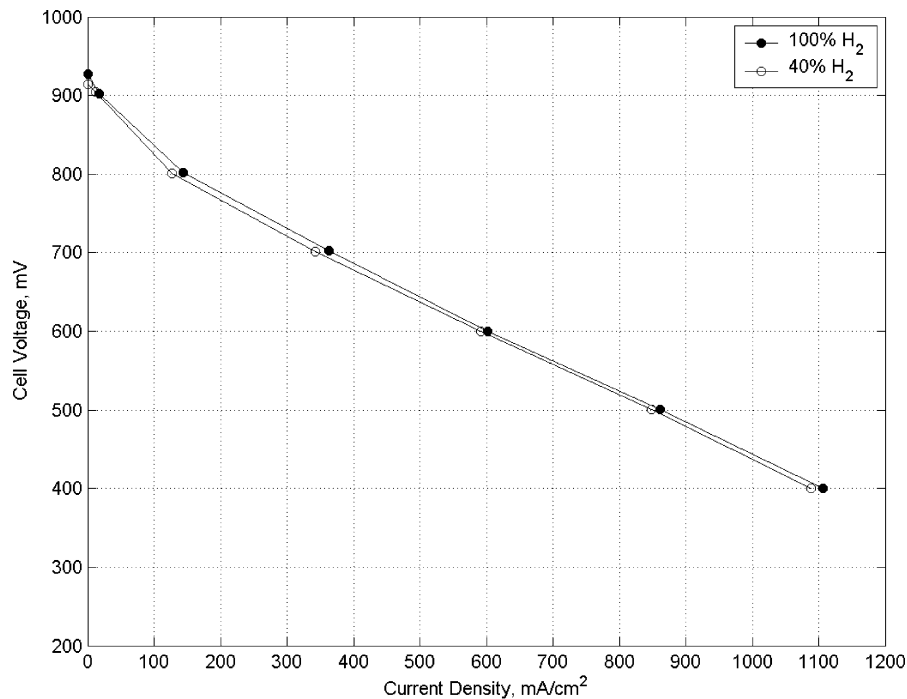


Fig. 1. Steady state cell polarization for 100% H₂ and 40% H₂ anode fed gas.

well as the calculated current from the model described by Eqs. (9)–(14). In all four cases, after the poisoning process was complete, the membrane was recovered by feeding the cell with a CO-free, 100% hydrogen anode feed for a period of 2 h. The current obtainable at 0.6 V during the recovery process for all four cases is shown in Fig. 7. For all cases,

the cell performance was revived after the poisoning process with the use of a pure hydrogen anode feed stream.

As shown in Figs. 2–5, the detrimental effects of CO can be measured even after just 10 min of exposure to the cell, with the fully poisoned steady state condition reached in roughly 120 min. It is clear from these polarization curves

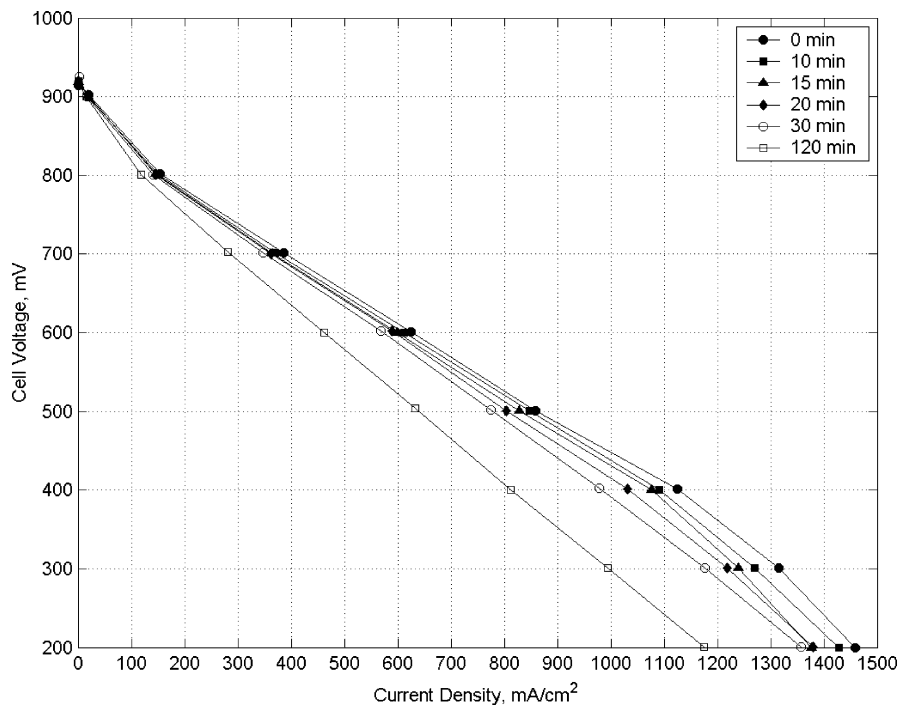


Fig. 2. Cell polarization at various time steps (in min) throughout the poisoning process, with 100% H₂, 10ppm CO anode feed.

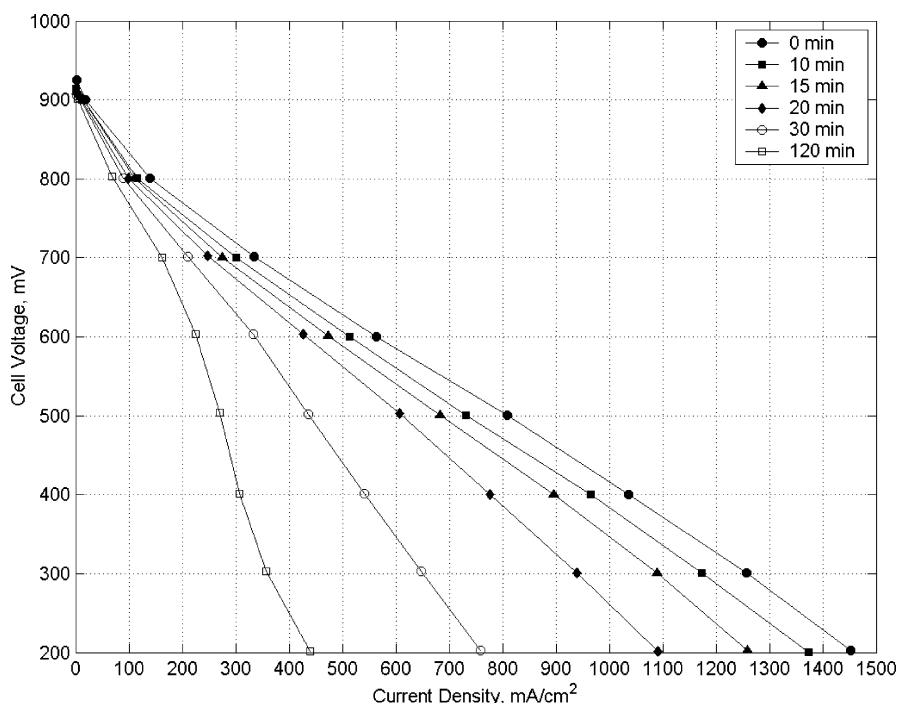


Fig. 3. Cell polarization at various time steps (in min) throughout the poisoning process, with 40% H₂, 10 ppm CO anode feed.

that while the presence of 10 ppm CO in 100% hydrogen has a noticeable effect (Fig. 2), 10 ppm CO in 40% hydrogen has an extremely detrimental effect (Fig. 3). The same is true at the 100 ppm level (Figs. 4 and 5). Fig. 6, which plots the current at a cell voltage of 0.6 V versus time, shows the transient performance drop for all four cases very clearly. At 10 ppm of CO in a 100% hydrogen fed stream, the steady

state current obtainable is 26% less than that before the poisoning process began. With 40% hydrogen and 10 ppm CO, the drop is 60%. At the 100 ppm level, the respective drops in current for 100% versus 40% hydrogen are 67 and 86%, respectively.

It was experimentally observed that while hydrogen dilution alone has almost no effect on cell performance, and

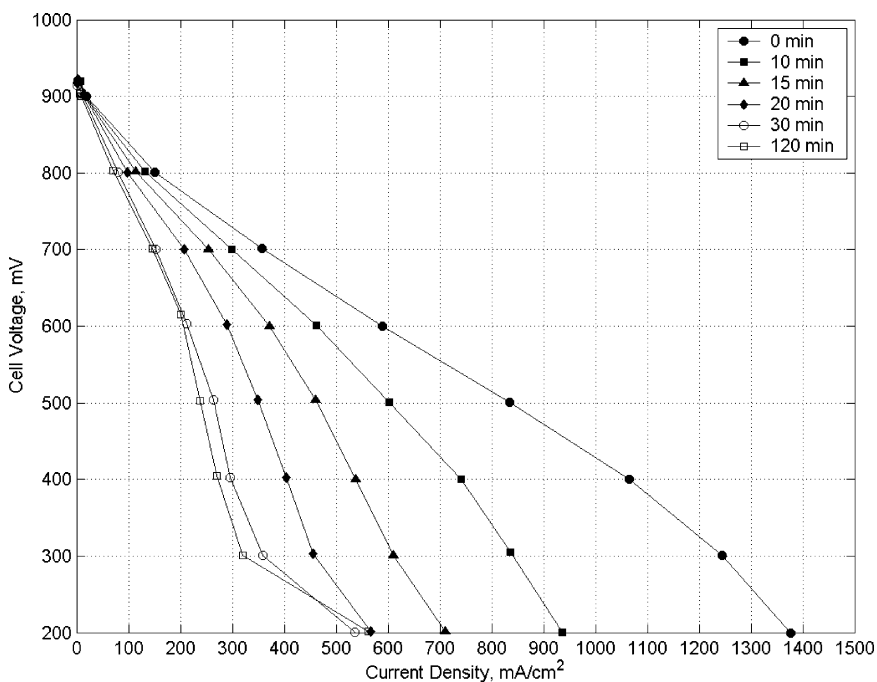


Fig. 4. Cell polarization at various time steps (in min) throughout the poisoning process, with 100% H₂, 100 ppm CO anode feed.

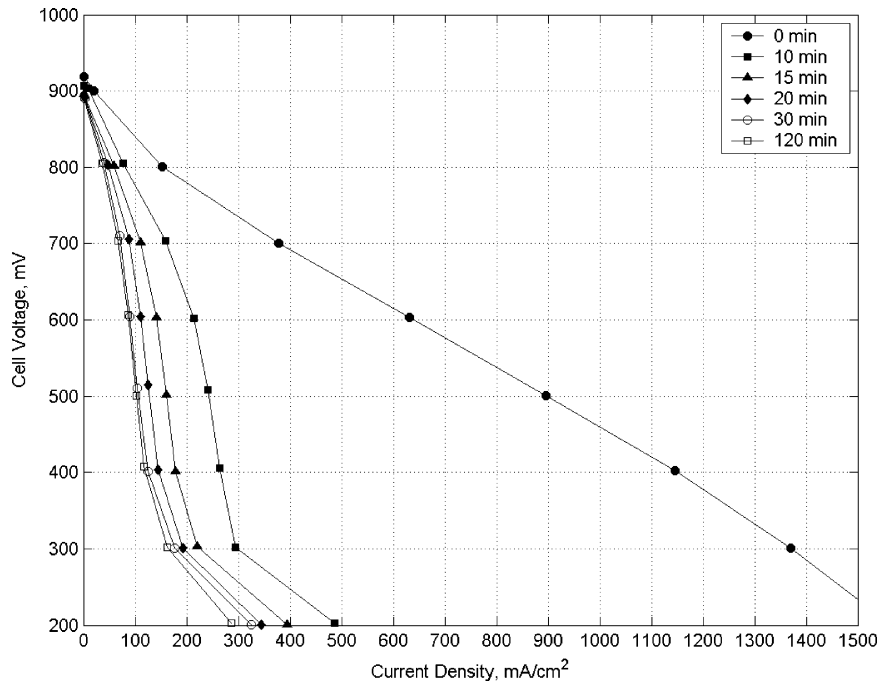


Fig. 5. Cell polarization at various time steps (in min) throughout the poisoning process with, 40% H₂, 100 ppm CO anode feed.

CO alone has a detrimental effect on cell performance, the combined effects of trace quantities of CO and hydrogen dilution have an extremely detrimental effect. This can be explained using the zero-dimensional model developed earlier.

Under normal cell operating conditions with pure hydrogen, the anode kinetic losses, η_a , are very low as compared to the kinetic losses at the cathode and the ohmic losses through the membrane. These normally small anode losses are given

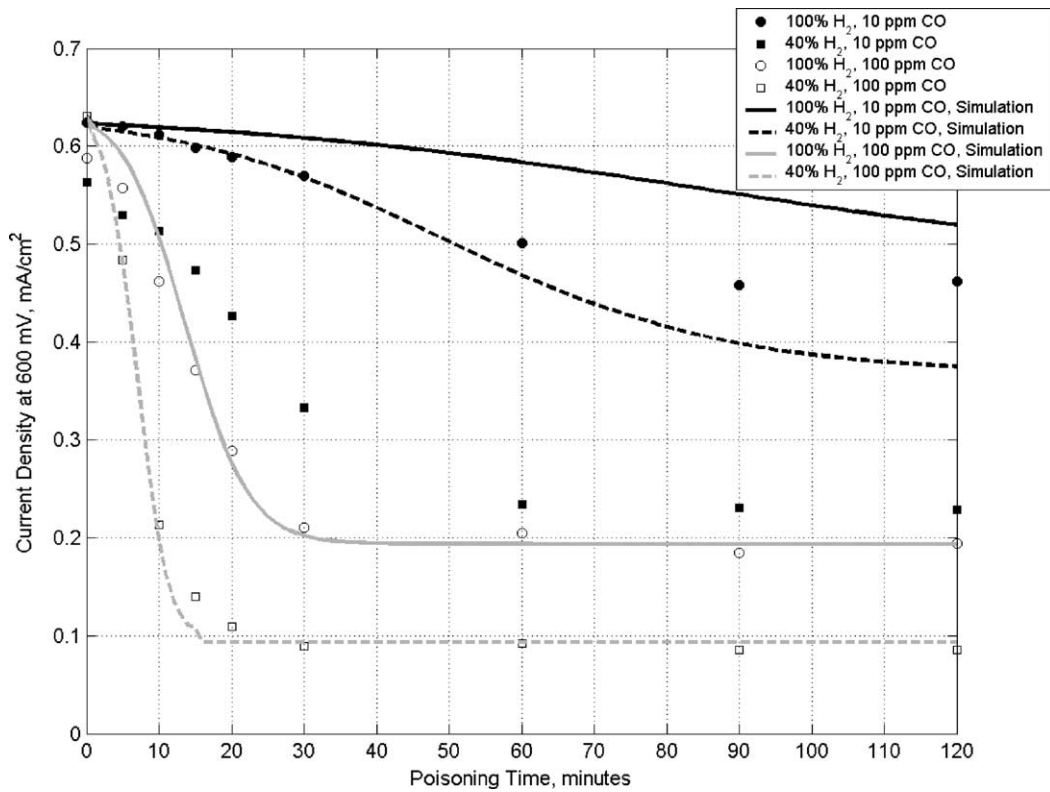


Fig. 6. Current at 0.6 V during the poisoning process vs. time for all four different anode feed gas compositions. The points represent actual experimental results, and the curves represent simulations based on the model developed.

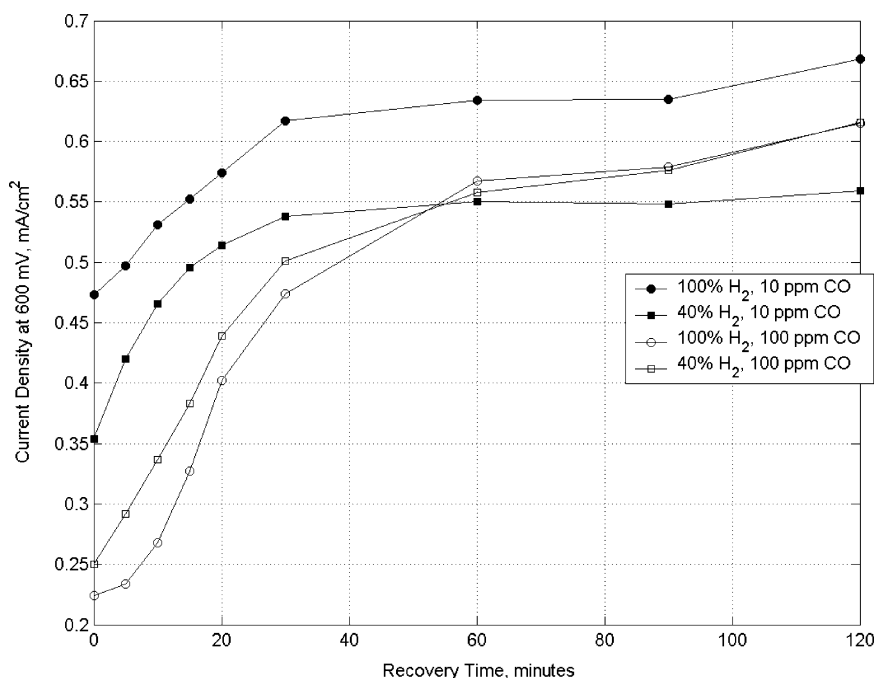


Fig. 7. Current at 0.6 V during the recovery process vs. time.

by Eq. (12), and are a function of fractional surface coverage of hydrogen, θ_h . Because θ_h appears in the denominator of an inverse hyperbolic sine relationship, the hydrogen fractional coverage must be very low for the anode overpotential losses to have a significant detrimental effect on cell performance. Thus, dilution alone, which reduces the hydrogen mole fraction, x_h in Eq. (9), and subsequently θ_h , does not have an appreciable effect on cell performance (Fig. 1).

The existence of CO in the anode feed stream, and its preferential adsorption on the catalyst surface, does have a substantial effect on cell performance. The presence of CO slows the hydrogen adsorption to such a degree that the fractional coverage θ_h falls by an order of magnitude, and thus the anode kinetic losses become significant in effecting overall cell voltage. Since the presence of CO reduces θ_h to a degree that the anode losses are now significant, hydrogen

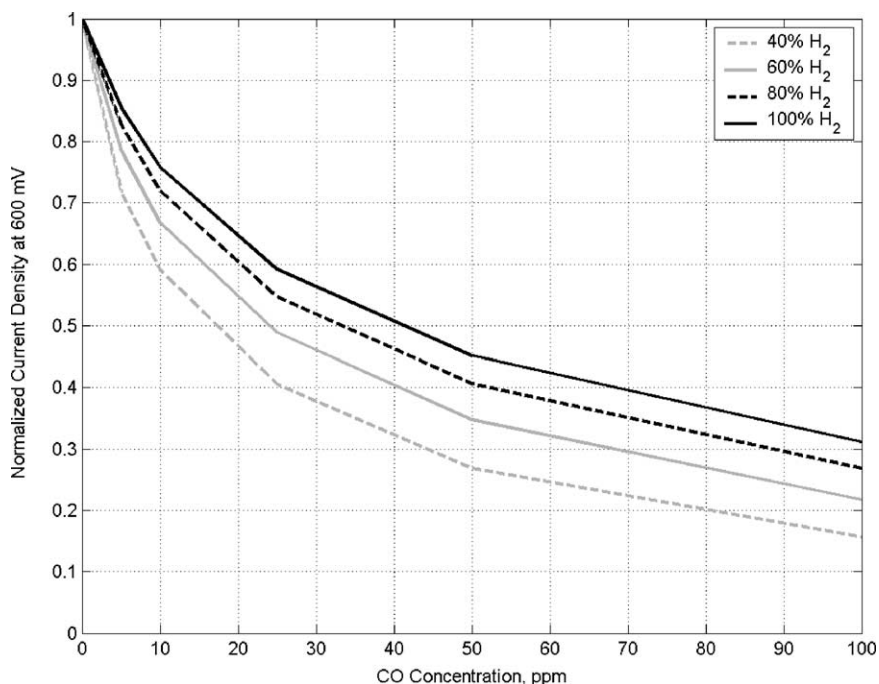


Fig. 8. Computed normalized steady state current at 0.6 V vs. CO concentration for various hydrogen dilution levels.

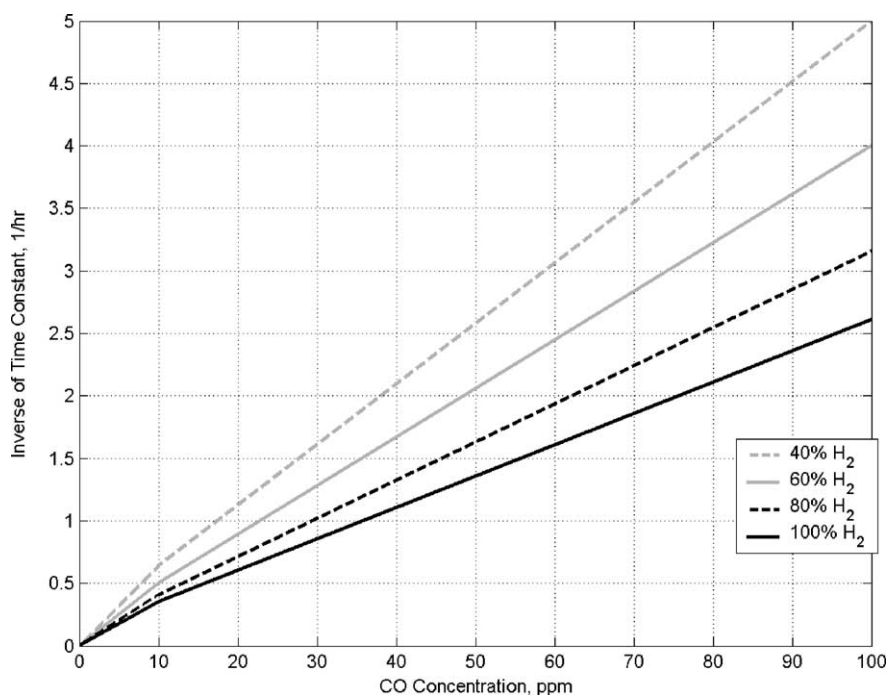


Fig. 9. Computed poisoning time constant vs. CO concentration for various hydrogen dilution levels.

dilution, which further reduces θ_h , now causes an additional decrease in cell performance.

This finding has enormous implications in terms of minimum purity requirements for anode feed gas. As Fig. 6 clearly illustrates, the commonly quoted number of 10 ppm CO as the limit for platinum catalyst based PEM fuel cells is highly dependent on the associated hydrogen dilution level of the feed gas. The performance loss from 40% hydrogen with 10 ppm CO is almost equal to the loss associated with 100% hydrogen and 100 ppm CO.

Although the simulation does not match the experimental data exactly for all cases, it does predict the general trend of transient poisoning, and demonstrates the combined effects that hydrogen dilution and CO can have on the cell performance. The discrepancies between the data and the simulation can be attributed to various causes. First, the CO poisoning model here is coupled with a zero-dimensional fuel cell performance model. Thus, no consideration is given for the spatial variations in fuel cell performance resulting from gradients in hydrogen, CO, water, and oxygen concentration that may exist within the cell flow field and the gas diffusion layer. Secondly, as mentioned earlier, the CO poisoning model here assumes the CO electro-oxidation term to be negligible as compared to CO surface adsorption and desorption terms. While true for low anode overpotential values, this assumption becomes less valid as the anode overpotential rises. This may explain to some degree the steady state error between the data and model. Lastly, the model is highly dependent on the hydrogen and CO adsorption, desorption, and electro-oxidation parameters chosen. Exact values for these parameters are unknown, and vary from electrode to electrode. Also, as noted earlier, several

of these parameters are believed to vary with the fractional CO coverage rather than being constant, as assumed here. Despite these drawbacks, the model still predicts the profile of the resulting current versus time curve of the transient poisoning process, as well as simulates the mutually detrimental effects that CO and dilute hydrogen can have.

Using the model, simulation of cell behavior under a host of different hydrogen dilution levels and CO concentrations is possible. Two of these such parametric simulations are shown in Figs. 8 and 9. The first shows the steady state current obtainable at a cell voltage of 0.6 V versus CO concentration. The current has been normalized with respect to the maximum current obtainable with CO-free feed gas. This is plotted for various hydrogen dilution levels. Fig. 9 compares the time constant for the poisoning process, for various hydrogen dilution levels, versus CO concentration. This time constant was found by calculating the period required for the cell current to suffer 90% of its steady state losses. The inverse of this time constant is plotted versus CO concentration in Fig. 9. Thus, a condition that poisons the cell faster has a higher inverse of time constant. The CO-free cases never get to a poisoned state, and thus takes infinite time. Consequently, the CO-free condition has an inverse time constant equal to zero. Figs. 8 and 9 reinforce the finding that hydrogen concentration has an effect on both the extent and the rate of CO poisoning.

5. Conclusion

The transient polarization of a PEM fuel cell undergoing the CO poisoning process has been experimentally

measured. This process was observed under variable CO and hydrogen dilution levels. The transient poisoning model developed by Springer et al. [5], which was modified and solved here, agrees well with the experimentally observed results of transient CO poisoning for both pure and dilute hydrogen feed streams.

It was found that while hydrogen dilution alone lowers the fractional coverage on the catalyst surface, it is only when CO is present that the coverage is lowered to a degree that affects cell voltage. Under this condition, the addition of hydrogen dilution will compound the low surface coverage problem even further, and thus cause very poor cell performance. Even with low CO levels normally considered safe for cell operation (i.e. 10 ppm), hydrogen dilution can cause an extremely severe loss of cell polarization. These results are easily explainable by the hydrogen and CO adsorption, desorption, and electro-oxidation model developed.

Acknowledgements

The authors would like to thank the United States Department of Energy, under cooperative agreement #DE-FC26-01NT41098, the ConocoPhillips Company, and the National Science Foundation for sponsoring this work.

Appendix A. Nomenclature

b_{fc}	backwards forward ratio of CO adsorption (atm)
b_{fh}	backwards forward ratio of hydrogen adsorption (atm)
F	Faraday's constant (96485 C mol^{-1})
i	current (A cm^{-2})
i_{oc}	cathode exchange current density (A cm^{-2})
k_{ec}	rate constant of CO electro-oxidation (A cm^{-2})
k_{eh}	rate constant of hydrogen electro-oxidation (A cm^{-2})
k_{fc}	rate constant of CO adsorption ($\text{A cm}^{-2} \text{ atm}^{-1}$)

k_{fh}	rate constant of hydrogen adsorption ($\text{A cm}^{-2} \text{ atm}^{-1}$)
P	total pressure (atm)
R	universal gas constant ($8.314 \text{ J mol}^{-1} \text{ K}^{-1}$)
R_{ohmic}	cell ohmic resistance ($\Omega \text{ cm}^2$)
t	time (s)
T	temperature (K)
V_{cell}	cell voltage (V)
V_o	open circuit voltage (V)
x_c	CO mole fraction
x_h	hydrogen mole fraction
α	charge transfer coefficient
η_a	anode surface overpotential (V)
η_c	cathode surface overpotential (V)
η_{ohmic}	ohmic voltage loss (V)
θ_c	fractional surface coverage of carbon monoxide
θ_h	fractional surface coverage of hydrogen
ρ	molar area density of catalyst sites times Faraday's constant (C cm^{-2})

References

- [1] Kirk-Othmer Encyclopedia of Chemical Technology, fourth ed., New York, 852, 1996.
- [2] L. Brown, *Int. J. Hydrogen Energy* 26 (2001) 381.
- [3] S. Um, C.Y. Wang, K.S. Chen, *J. Electrochem. Soc.* 147 (2000) 4485.
- [4] S. Gottesfeld, J. Pafford, *J. Electrochem. Soc.* 135 (1988) 2651.
- [5] T.E. Springer, T. Rockward, T.A. Zawodzinski, S. Gottesfeld, *J. Electrochem. Soc.* 148 (2001) A11.
- [6] J. Divisek, H. Oetjen, V. Peinecke, V. Schmidt, U. Stimming, *Electrochim. Acta* 43 (1998) 3811.
- [7] S.H. Chan, S.K. Goh, S.P. Jiang, *Electrochim. Acta* 48 (2003) 1905.
- [8] J. Zhang, T. Thampan, R. Datta, *J. Electrochem. Soc.* 149 (2002) A765.
- [9] H. Oetjen, V. Schmidt, U. Stimming, F. Trila, *J. Electrochem. Soc.* 143 (1996) 3838.
- [10] M. Murthy, M. Esayian, A. Hobson, S. MacKenzie, W. Lee, J. Van Zee, *J. Electrochem. Soc.* 148 (2001) A1141.
- [11] N. Wagner, Schulze, *Electrochim. Acta* 48 (2003) 3899.